

Laser System for a Compton Polarimeter

Ken Moffeit and Mike Woods
SLAC

Abstract:

We describe the Laser System for a Compton Polarimeter for the NLC-500 Linear Collider Design.

1. Introduction

The primary beam polarization measurement at a future Linear Collider (LC) will be by a Compton polarimeter.[1,2,3] In the NLC-500 design, this polarimeter is located in the extraction line approximately 60 meters downstream from the Interaction Point[1,2]. Advantages of Compton polarimetry for precise polarization measurements at the LC are discussed in reference [2]. Advantages for a polarimeter downstream of the IP relative to an upstream polarimeter are also discussed there.

The location in the extraction line is shown in Figure 1. It is at a secondary focus in the middle of a chicane with 20 mm dispersion, but with no net bend angle with respect to the e^- direction at the primary e^+e^- IP.[4] At the middle of the chicane the Compton scattering occurs and the scattered electrons are confined to a cone having a half-angle of $\theta = 2 \mu\text{rad}$, effectively collinear with the initial electron direction.

2. Light source

The Compton laser light source provides high-intensity pulses of circularly polarized light at the Compton Interaction Point, CIP. The laser beam must be transported with minimal loss of polarization from the laser source to the collision point with the electrons. The systems of the Compton laser light source are shown in Figure 2. The circular polarization of the light must be well measured and monitored to achieve an uncertainty in the circular polarization of the laser light at the Compton IP of 0.1%. The light source for the Compton polarimeter for NLC described here is similar to that used in the SLD experiment at the SLAC Linear Collider[5].

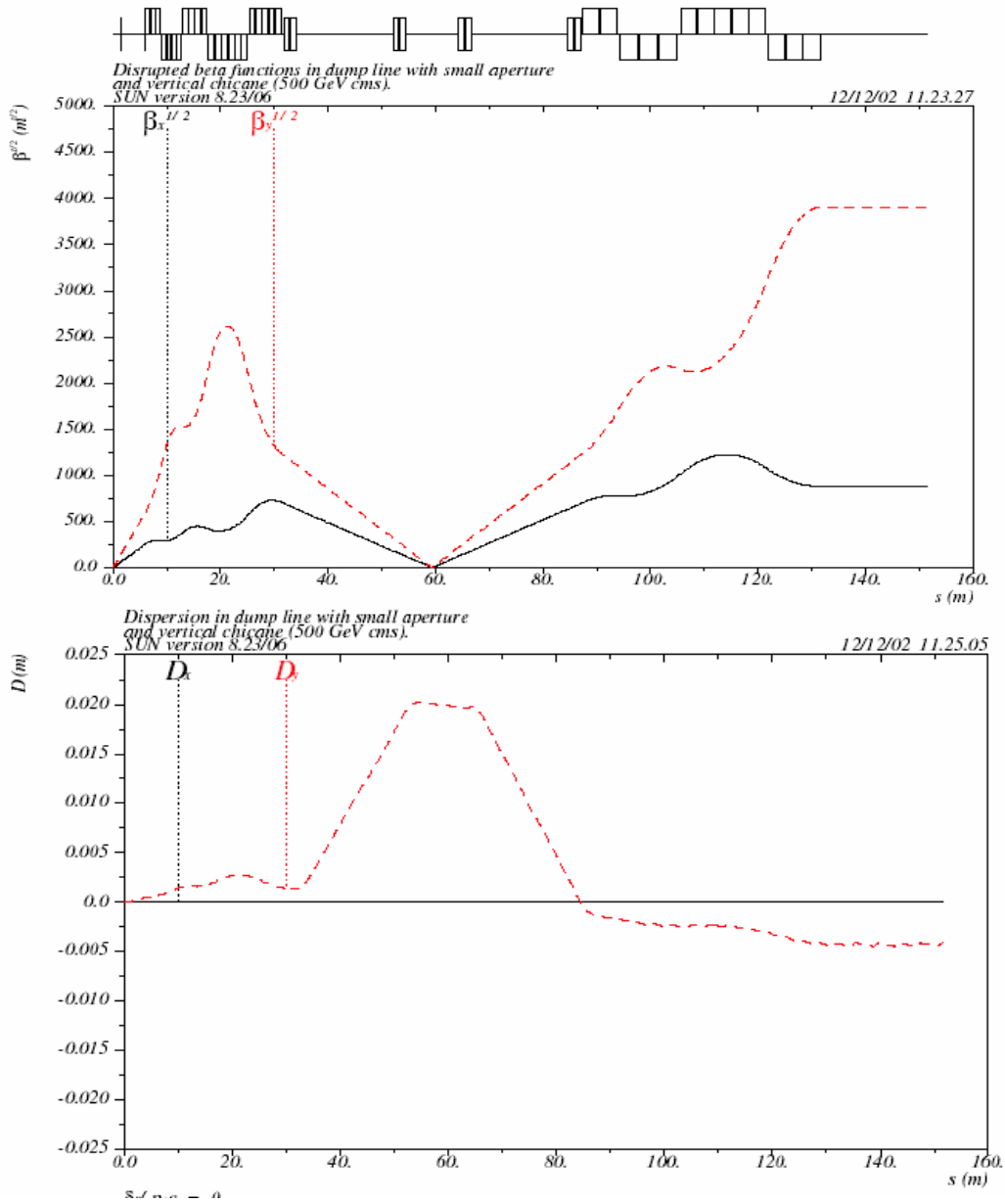


Figure 1: Beta-functions and dispersion in the extraction line as a function of distance from the IP. The Compton Interaction Point is located at the secondary focus approximately 60 meters downstream.[4]

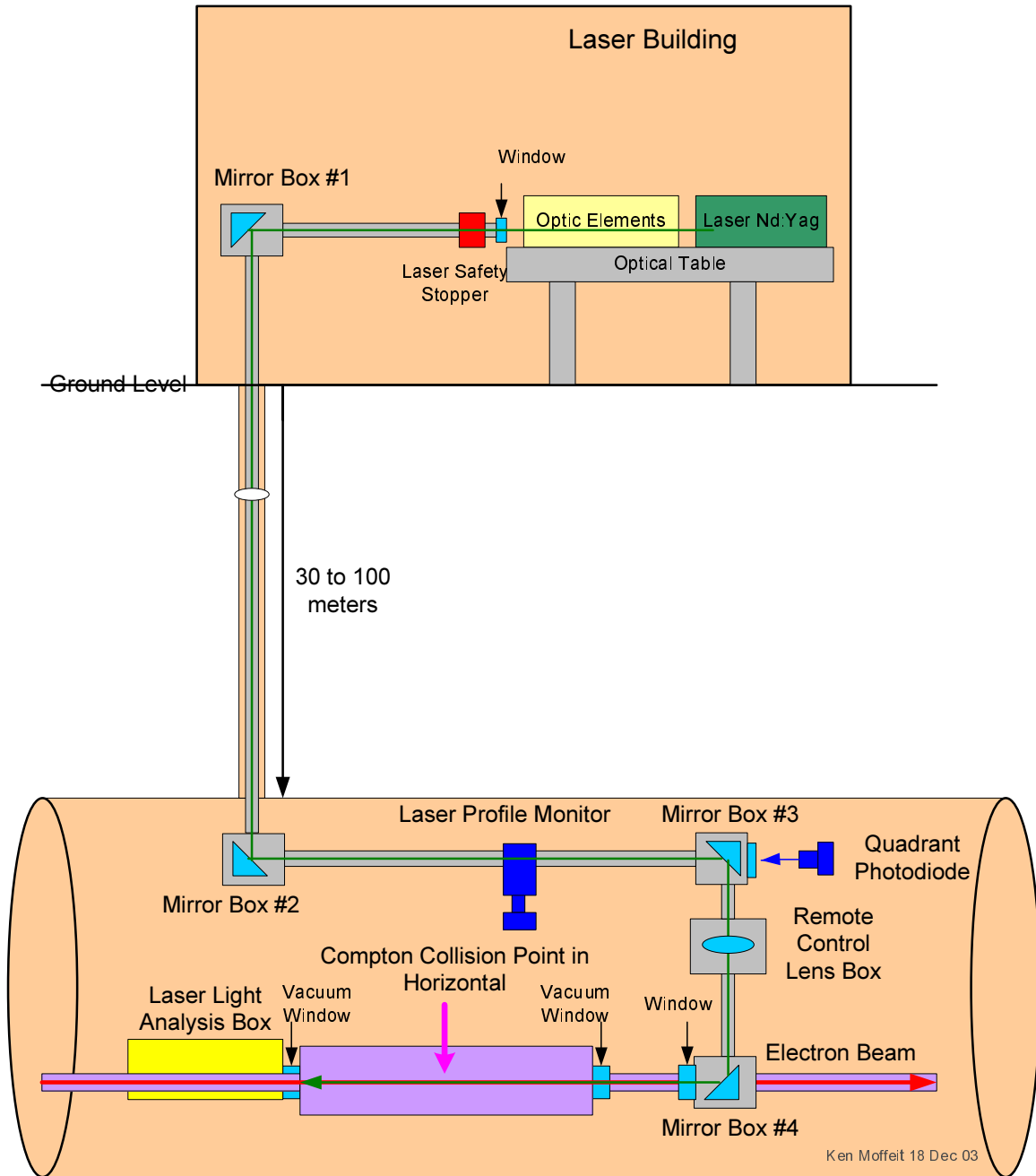


Figure 2: Schematic of the systems of the Compton laser light source showing the laser and optics above ground, the transport line to the Compton Interaction Point in the tunnel underground and the Analysis Box.

The laser bench, holding the laser and optics, is shown in Figure 3. It is located above ground in a building situated above the Compton Interaction Point in the extraction line tunnel.

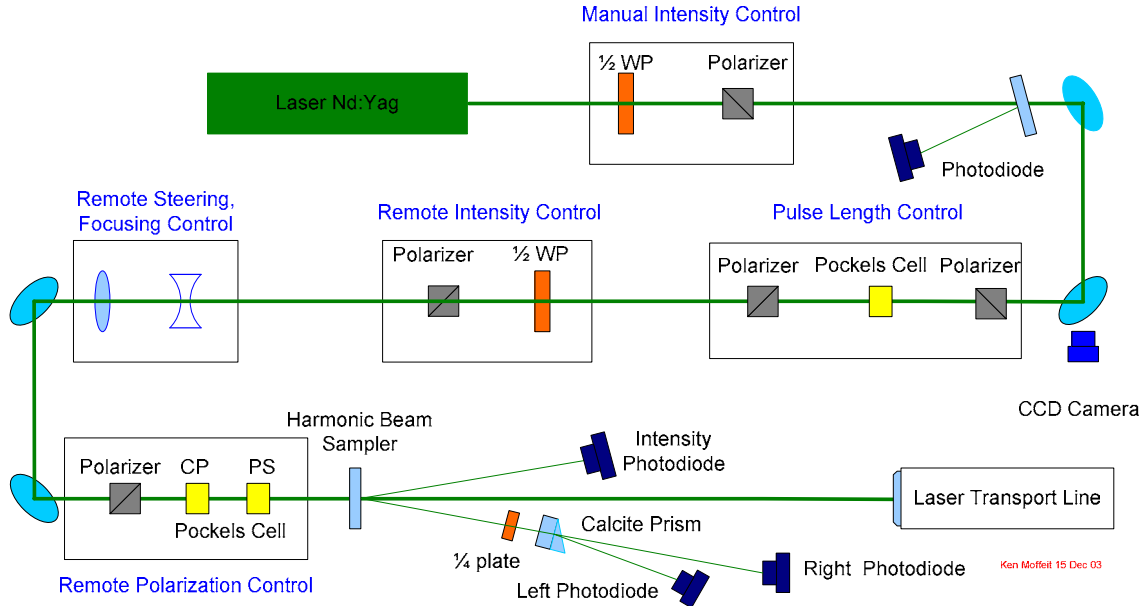


Figure 3: Diagram of the Compton source laser optical bench layout.

2a. Laser

A frequency doubled Nd:YAG (Neodymium:Yttrium-Aluminum-Garnet) laser is used with a wavelength of 532 nm (2.33 eV). The solid Nd:YAG rod is pumped into an excited state by flash lamps, and the resulting atomic transitions produce 1064 nm photons. The beam passes through a frequency-doubling crystal, which uses a nonlinear optics phenomenon to combine two 1064 nm photon states into a single 532 nm state. The resulting beam of 1064 nm and 532 nm photons passes through an infrared separator to assure that there are only 532 nm photons in the laser beam as it enters the optics bench optical components. The laser fires on every 7th pulse train of the 120 Hz repetition rate of the electron beam, but every 10 seconds fires instead on the 6th pulse train; this gives an average repetition frequency of ~17 Hz. The laser pulse energy delivered to the Compton IP is ~100 mJ. The duration of the Q-switched laser pulse is ~6 nanoseconds. The light emerges from the laser linearly polarized. A possible available commercial laser is the Continuum Powerlite Model 8020: 20Hz; 550 mJ at 532nm; 6ns pulsewidth (FWHM)[6].

2b. Manual Laser Intensity Control

A manually adjusted $\frac{1}{2}$ -wave plate, in conjunction with a linear polarizer, attenuates the beam to the desired intensity to avoid damaging optical components on the bench and in the transport line. A photodiode sees a small reflected beam from an optical flat and monitors the output of the laser. If the output drops below the dynamic range of the Remote Intensity Control the operator manually adjusts the first $\frac{1}{2}$ -wave plate or does maintenance on the laser, e.g. changes flash lamps. A set of dielectric mirrors directs the laser beam to the pulse length control system, remote intensity control system and the remote steering/focusing control optical elements. A CCD camera monitors the laser spot looking at the transmitted light through the second nearly-100% reflecting mirror.

2c. Pockels Cell

A number of Pockels cells are used in the optical systems to obtain a short pulse and to circularly polarize the laser light. The Pockels cell was invented by Friedrich Pockels in 1893. A Pockels cell alters the polarization state of light passing through it when an applied voltage induces birefringence changes in an electro-optic crystal such as KD*P. When used in conjunction with polarizers, these cells can function as optical switches, or laser Q-switches. It is a voltage-dependent optical compensator inducing different phase shifts along different axes. The fast axis has the smallest phase shift, and the axis perpendicular is the slow axis and has the largest phase shift. The axes of the Pockels cell are aligned 45 degrees to the linear polarization of the incident light. The specifications for the Pockels cell give the high voltages, which corresponds to a quarter-wave and half-wave shift of the wavelength of the incident light. Circularly polarized light is obtained by setting a voltage on the electrodes of the Pockels cell corresponding to a quarter-wave shift. Changing the sign of the voltage allows one to switch from right-circularly polarized light to left-circularly polarized light. The type of Pockels cell used in the SLD Compton Laser System for generating circular polarization is shown in Figure 4.

2d. Laser Pulse Length

A Pockels Cell is sandwiched between two crossed linear polarizers. A fast pulser drives the Pockels Cell at the $\frac{1}{2}$ -wave voltage thereby rotating the linear polarization 90 degrees. The second crossed linear polarizer then accepts the laser light rotated and filters the non-rotated light. A narrow laser pulse length of ~ 2 nsec can be achieved. This narrow laser pulse ensures that only a single bunch of the electron beam pulse train is in collision. The timing of the Q-switched laser pulse and the fast pulser with respect to the electron beam pulse allows the polarization of each bunch of the electron beam pulse train to be measured.

2e. Remote Intensity Control

The Remote Intensity Control consists of a remotely adjustable $\frac{1}{2}$ -wave plate and linear polarizer and is used to remotely adjust the laser beam intensity to maintain the desired light intensity at the Compton IP.

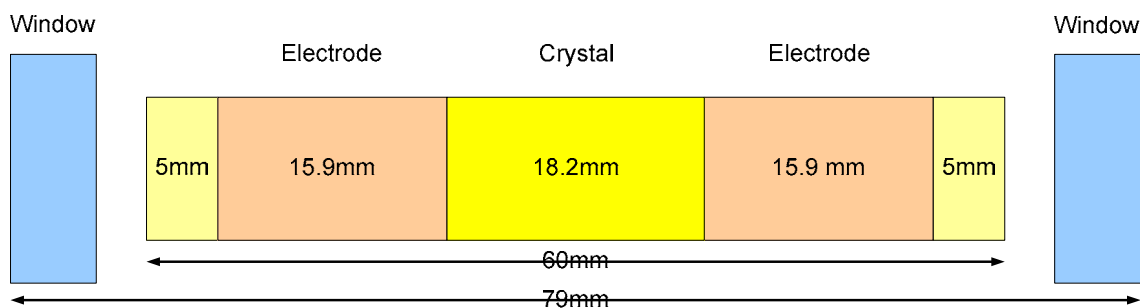


Figure 4: Cleveland Crystals Model TX3460 Pockels cell.

2f. Remote Steering and Focusing Control

The beam is expanded to 2-cm diameter to reduce the intensity on the optics and provide a collimated beam through the transport line to the Compton IP, between 30 and 100 meters underground. The lenses are mounted on a remotely movable stage with motion transverse to the beam. The laser beam position in the transport line is controlled remotely with this motion. Using a quadrant photodiode behind Mirror Box 3 (see Figure 2) for the steering diagnostic, the laser spot at the Lens Box can be maintained. The distance between the lenses can be adjusted to control the collimated beam profile in the transport line.

2g. Remote Polarization Control

A second set of dielectric mirrors directs the laser beam to the laser transport line for transport to the Compton IP. Another linear polarizer follows to ensure 100% linear polarization as the laser beam enters the Remote Polarization Control. The beam enters a set of two Pockels cells to create circularly polarized light at the Compton IP. The first Pockels cell labeled CP produces the desired circular polarization and is operated pulse-by-pulse with a pseudo-random helicity selection. It is referred to as the Circular Polarization Pockels cell because when the linear polarized light passes through it, it

becomes almost completely circularly polarized. The principle axes of this cell are tilted by 45° with respect to the linear polarization of the incident light. The second Pockels cell provides phase adjustment so the beam can be made nearly 100% circularly polarized at the Compton IP. The phase adjustment is needed to compensate for effects from the optical elements in the transport line. The principle axes of this cell are either parallel or perpendicular to the axes defined by the initial linear light. Thus the retarding axes of the PS Pockels cell are aligned 45° with respect to the axes of the CP Pockels cell.

After exiting the Pockels cell, the beam is separated by a harmonic beam sampler giving two new beams at 10 degrees (each with $\sim 1\%$ of the intensity of the primary beam), while the primary beam continues into the laser transport line. One of the beams from the harmonic beam sampler is directed into a photodiode to monitor the laser intensity. The other beam enters a helicity filter consisting of a quarter-wave plate and calcite prism. The calcite prism separates the two perpendicular light polarization components and directs them into two photodiodes. These photodiodes monitor the circular polarization of the light, P_γ , as it enters the transport system through the following relation

$$P_\gamma = \frac{R - L}{R + L}, \tag{1}$$

where R, L are the (appropriately normalized) signals of the *Right, Left* photodiodes.

The crystal of a calcite prism has an index of refraction of 1.49 (1.66) for linear polarization in (perpendicular to) the scattering plane. Figure 5 shows the calcite prism used as a helicity filter.

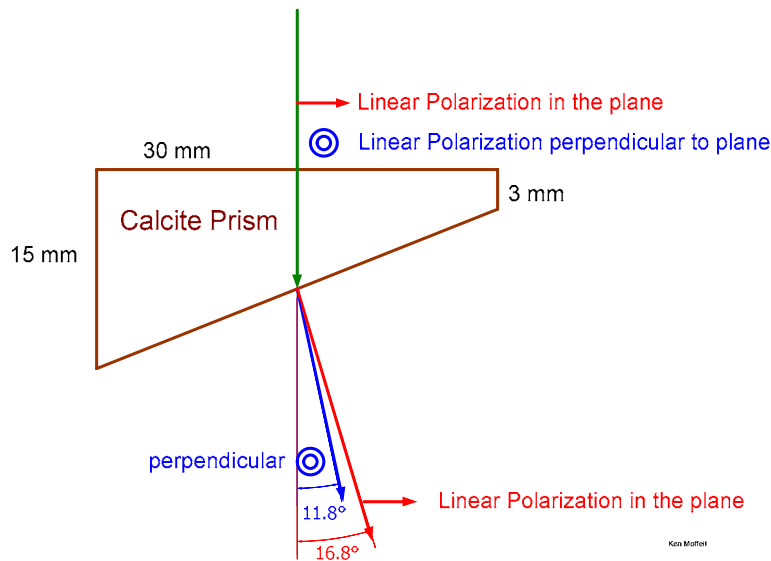


Figure 5: Diagram of Calcite Prism used in Helicity Filter.

By varying the voltages on the CP and PS Pockels cells maximal circular polarization (~99.9%) at the Compton IP can be achieved. The electric field vector after the PS cell in Jones Matrix notation is given by:

$$|E\rangle = \begin{pmatrix} E_x \\ E_y \end{pmatrix} = e^{i(\pi/2 + \delta_{PS})} \begin{pmatrix} \sin\left(\frac{\delta_{CP}}{2}\right) \\ \cos\left(\frac{\delta_{CP}}{2}\right) \end{pmatrix} \quad (2)$$

where

$$\delta_{CP} = \frac{V_{CP}}{V_{CP}^{\lambda/4}} \cdot \frac{\pi}{2}$$

$$\delta_{PS} = \frac{V_{PS}}{V_{PS}^{\lambda/4}} \cdot \frac{\pi}{2}$$

and V_{CP} (V_{PS}) is the CP (PS) Pockels Cell voltage, $V_{CP}^{\lambda/4}$ ($V_{PS}^{\lambda/4}$) is the CP (PS) quarterwave voltage. V_{CP} controls the relative amplitudes of the E_x and E_y components and V_{PS} controls their relative phase. Hence, arbitrary elliptical polarization can be generated with this configuration. The Stokes parameters for the laser polarization following the PS cell are:

$$\begin{aligned} s_1 &= \cos\left(\frac{\delta_{CP}}{2}\right) = \frac{X - Y}{X + Y} \\ s_2 &= \sin(\delta_{CP}) \sin(\delta_{PS}) = \frac{U - V}{U + V} \\ s_3 &= \sin(\delta_{CP}) \cos(\delta_{PS}) = \frac{R - L}{R + L} \end{aligned} \quad (3)$$

$$(s_1^2 + s_2^2) + s_3^2 = L^2 + C^2 = 1 \quad (4)$$

where s_1 and s_2 describe the linear polarization components and s_3 is the circular polarization. For polarized light, the linear and circular polarization components add in quadrature to 1. The CP and PS Pockels cells allow for compensating imperfections in the polarization Pockels cells and for phase shifts in downstream optics before the Compton IP. The circular polarization at the Compton IP is given by:

$$\begin{aligned}
s_3(CIP) &= \sin(\delta_{CP} + \delta_{CP}^{CIP}) \cos(\delta_{PS} + \delta_{PS}^{CIP}) \\
&= \sin\left(\frac{V_{CP} + \delta V_{CP}^{CIP}}{V_{CP}^{\lambda/4}} \cdot \frac{\pi}{2}\right) \cos\left(\frac{V_{PS} + \delta V_{PS}^{CIP}}{V_{PS}^{\lambda/4}} \cdot \frac{\pi}{2}\right) \quad (5)
\end{aligned}$$

where δ_{CP}^{CIP} and δ_{PS}^{CIP} describe the Pockels cell imperfections and phase shifts in the laser transport optics.

3. Transport Line

The transport line is designed to direct the laser light to the Compton IP with minimal alteration of the circular polarization. A schematic of the transport line is shown in Figure 2. The laser beam enters the transport line through a window of negligible birefringence and passes a fail-safe laser stopper located inside the laser building. The laser stopper is part of the laser safety system and does not allow laser light downstream when there is an unsafe condition, e.g. when the transport line is not at proper pressure. The transport line is filled with 3-5 psi overpressure of filtered nitrogen, in order to minimize optics damage.

The beam undergoes four sets of matched circular polarization preserving pairs of mirrors. By using identical dielectric mirrors manufactured at the same time, any relative phase shift for “s” and “p” polarization states (out-of-plane and in-plane polarization states) introduced by the first mirror is exactly compensated for and removed by the second mirror in each Mirror Box. The two paired mirrors of each Mirror Box reflect the beam perpendicular to each other, resulting in a laser beam with “s” polarization at the first mirror becoming “p” polarized for the 2nd mirror and vice versa. For example, the first mirror of Mirror Box(1) reflects the beam 90 degrees in the horizontal and the second reflect the beam 90 degrees to the vertical down the shaft.

Before the beam arrives at Mirror Box (4) it enters a Lens Box. Here it is focused at the Compton IP with a lens of 10m focal length. The lens can be moved remotely in the two horizontal directions allowing the laser beam to be steered into collisions with the electrons. It is important that the laser spot be centered on the nominal position of the lens. Movement of the mirror boxes due to temperature variation throughout the day may cause the laser spot to move at the Lens Box. A quadrant photodiode behind Mirror Box (3) can be used as the diagnostic for a steering feedback using the Remote Steering Control on the Optical Bench in the Laser Building above ground (see Figure 3) to keep the laser spot in the desired position at the Lens Box.

After the final Mirror Box (4) the laser light exits the transport line through an optical window with negligible birefringence. The laser beam then enters the extraction line vacuum through a 2-inch optical window with negligible birefringence. As seen in Figure 6 the laser light crosses the electron beam in the horizontal at an angle of 11.5 mrad. The focusing of the laser optics are chosen to achieve a laser waist at the Compton IP with an RMS spotsize of 100 μm .

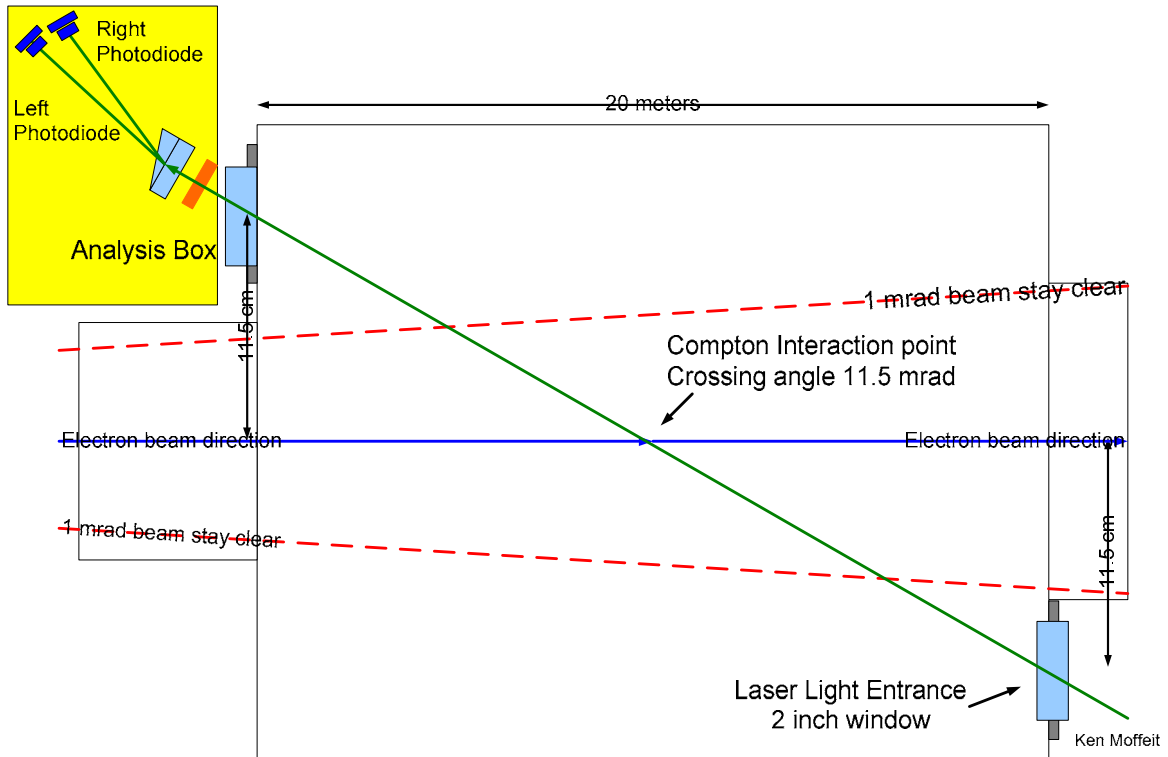


Figure 6: Plan view of the laser light path through the Compton interaction point. The crossing angle is 11.5 mrad. The circular polarization of the laser light is measured in the Analysis Box. Also shown is the 1mrad beam stayclear with respect to the e^+e^- IP, allowing clearance for the beamsstrahlung photons.

The photons exit the extraction line vacuum through a 2" window with negligible birefringence. The laser light enters an Analysis Box where a $\frac{1}{4}$ -wave plate, calcite prism and (quadrant) photodiodes measure the circular polarization (see Figure 7). Quadrant photodiodes can be used for a 2nd remote steering feedback, using the Lens Box for the steering control. This, together with the steering feedback to stabilize the laser beam at the Lens Box, stabilizes the laser trajectory at the Compton IP.

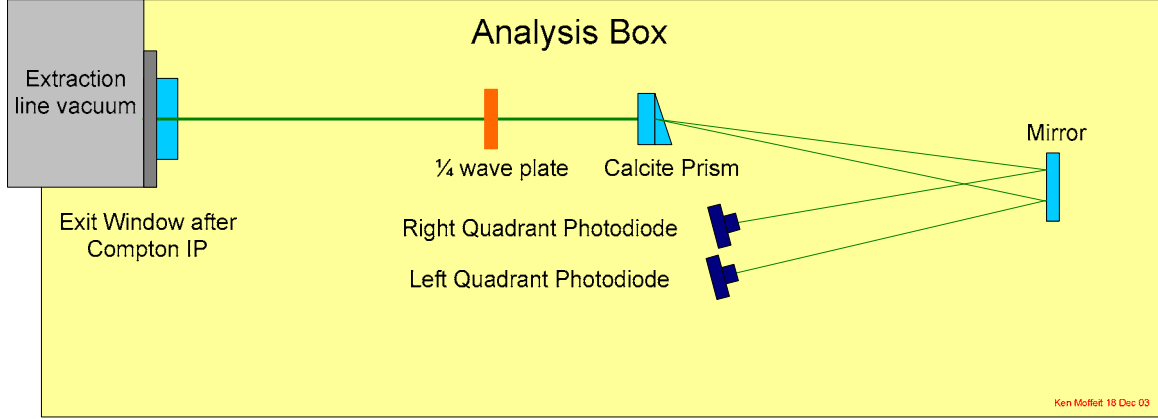


Figure 7: The Analysis Box optics located after the Compton IP.

4. Laser Beam Polarization Measurement at the Compton IP

The laser circular polarization, P_γ , at the Compton IP is determined from photodiode measurements of the laser beam and from Compton asymmetry measurements of the beam electrons Compton-scattered from the laser beam. The laser polarization is directly measured before and after the Compton IP by measuring the amount of left-polarized and right-polarized light, using the *Right* and *Left* photodiodes that follow an helicity filter. The Compton asymmetry measurement is defined to be

$$A_{Compton} = \frac{N^{\rightarrow\rightarrow} - N^{\rightarrow\leftarrow}}{N^{\rightarrow\rightarrow} + N^{\rightarrow\leftarrow} - 2N^{off}} = AP_{Compton} \cdot P_e P_\gamma \quad (6)$$

where $N^{\rightarrow\rightarrow}$ ($N^{\rightarrow\leftarrow}$) is the detector signal for electron and laser photon spins aligned (anti-aligned); N^{off} is the detector signal with electron beam present, but no laser beam; $AP_{Compton}$ is the analyzing power calculated from the Compton cross section and the detector response function; P_e is the electron beam longitudinal polarization; and P_γ is the laser beam circular polarization.

The *Right* (PD^+) and *Left* (PD^-) photodiode signals and the measured Compton asymmetry ($A_{Compton}$), are well-approximated by the following formulae:

$$PD^\pm = \frac{G^\pm}{2} \cdot \left[1 \pm \sin\left(\frac{V_{CP} + \delta V_{CP}^T}{V_{\lambda/4}^{CP}} \cdot \frac{\pi}{2}\right) \cos\left(\frac{V_{PS} + \delta V_{PS}^T}{V_{\lambda/4}^{PS}} \cdot \frac{\pi}{2}\right) + u \right] \quad (7)$$

$$A_{Compton} = P_e \cdot AP_{Compton} \cdot (1 - u) \cdot \sin\left(\frac{V_{CP} + \delta V_{CP}^{CIP}}{V_{\lambda/4}^{CP}} \cdot \frac{\pi}{2}\right) \cos\left(\frac{V_{PS} + \delta V_{PS}^{CIP}}{V_{\lambda/4}^{PS}} \cdot \frac{\pi}{2}\right)$$

where G is the photodiode gain; V_{CP} and V_{PS} are the Pockels cell voltages, $V_{\lambda/4}$ is the Pockels cell quarterwave voltage; δV_{CP}^T and δV_{PS}^T are the laser transport phase shifts to the photodiode diagnostics; u is the amount of unpolarized light; and δV_{CP}^{CIP} and δV_{PS}^{CIP} are the

laser transport phase shifts to the Compton IP. Measurements of PD^+ , PD^- and $A_{Compton}$ are made at different Pockels cell voltages (*Pockels cell scans*) to monitor the laser transport phase shifts and the Pockels cell quarterwave voltages. This was done for the SLD Experiment, which achieved $P_\gamma = (99.8 - 99.9)\%$ at the Compton IP with a systematic error of 0.1%. [5]

5. Compton Collision Rate

We plan to use a threshold Cerenkov detector, similar to that employed in the SLD Compton polarimeter [5,7]. It is a segmented electron detector sampling the flux of scattered electrons near the kinematic endpoint. It provides a good polarization measurement with high analyzing power. The counting rate per bunch crossing is:

$$R = R^0 \cdot \frac{l_{eff}}{l_{FWHM}} \quad (8)$$

where R^0 is the rate for headon collisions, l_{eff} is the length of the laser bunch that collides with the (smaller) electron beam due to the crossing angle and l_{FWHM} is the length of the laser bunch.

$$R = \sigma_{Compton} \cdot \frac{N_{electrons} \cdot N_{photons}}{\pi \sigma_y \cdot \sigma_x} \cdot \left[\frac{2.35 \sigma_x}{\tan \theta_{cross}} \cdot \frac{1}{l_{FWHM}} \right] \quad (9)$$

We use $N_{electrons} = 0.75 \times 10^{10}$; $N_{photons} = 2.7 \times 10^{17}$ (100 mJ of 2.33 eV photons); $\sigma_y = 100 \mu\text{m}$; $\theta_{cross} = 11.5 \text{ mrad}$; $l_{FWHM} = 0.6 \text{ m}$ (corresponding to 2ns pulse length); $\sigma_{Compton} = 2.25 \times 10^{-31} \text{ m}^2/\text{GeV}$ at the Compton endpoint (for an electron beam energy of 250 GeV and a laser photon energy of 2.33 eV). The counting rate is high with ~500 Compton electrons per GeV at the endpoint energy of 25.1 GeV. With the current extraction line geometry, this corresponds to:

$$R = \frac{600 \text{ scattered electrons}}{\text{cm}} \cdot \left(\frac{100 \mu\text{m}}{\sigma_y} \right) \cdot \left(\frac{11.5 \text{ mrad}}{\theta_{cross}} \right) \cdot \left(\frac{E_{laser}}{100 \text{ mJ}} \right) \cdot \left(\frac{2 \text{ n sec}}{t_{FWHM}} \right) \quad (10)$$

References

1. D. Cinabro, E. Torrence and M. Woods, "Status of (Next) Linear Collider Beam Instrumentation Design," LCD-ALCPG-03-0001 (2003).
<http://www.slac.stanford.edu/xorg/lcd/ipbi/notes/white.pdf>
2. K. Moffeit and M. Woods, document in preparation on NLC polarimeter for POWER document.
3. V. Gharibyan, N. Meyners and P. Schuler, LC-DET-2001-047, 2001.
4. Extraction line optics design has been done by Y. Nosochkov. See Y. Nosochkov, T.O. Raubenheimer, K. Thompson, and M. Woods,. SLAC-PUB-8096 (1999).
e-Print Archive: **physics/0106062**.
5. SLD Collaboration, Phys. Rev. Lett. **70**, 2515 (1993); SLD Collaboration, Phys. Rev. Lett. **86**, 1162 (2001); R. Elia, SLAC-Report-429 (1994); R. King, SLAC-Report-452, 1994; A. Lath, SLAC-Report-454, 1994; E. Torrence, SLAC-Report-509, 1997. The technical description of the laser light source for the SLD experiment found in the theses cited here have been used for some parts of this publication.
6. Description of Continuum Powerlite Laser found at
http://www.continuumlasers.com/pdfs/Powerlite_Prec_II_8000.pdf
7. M. Woods, SLAC-PUB-7319, 1996. e-Print Archive: **hep-ex/9611005**.